In vitro effect of AgNP nanoparticles on *Acanthamoeba castellani* parasite

Zainab S. Almayah, Intisar Albandar*& Shaimaa A. Alsamir

Department of Biology, College of Science, University of Basrah, Basrah, Iraq

***Corresponding author E-mail:** intisar.albandar@uobasrah.edu.iq

https://doi.org/10.29072/basjs.20260201

ARTICLE INFO

Received: 08 November 2025

Accepted: 23 April 2026

Published: 31 August 2026

Keywords:

Acanthamoeba castellani Nanotechnology, Silver nanoparticles, Antiparasitic nanoparticles, Rosmarinus officinalis

ABSTRACT

Keratitis is a vision-threatening corneal infection caused by the protozoan *Acanthamoeba castellani*, for which there is currently no viable and safe therapy in either people or animals. As a result, more effective and safer anti-amoebic agents are urgently needed. The study aims to determine the effect of silver nanoparticles (AgNPs) on clinical strains of *Acanthamoeba* spp. 78 *Acanthamoeba Keratitis* (AK) patients' corneal smear were collected using a sterile swab from different hospitals in Basrah province, Iraq. Silver nanoparticles (AgNPs) were synthesized using *Rosmarinus officinalis* leaf extract, and used with serial concentrations to evaluate their in vitro cytotoxicity. AgNPs exhibited an absorbance peak at 455 nm. The FTIR analysis identified the chemical constituents in the extract that contribute to AgNP synthesis and surface stabilization. AgNPs displayed a size of 25.70 nm and a Z-average of 106.3 nm using Zeta sizer. The X-ray diffraction (XRD) analysis was comparable to the positions of the standard of Ag and AgO. Zeta potential analysis revealed a peak at -41.7 mV. Field Emission Scanning Electron Microscope (FE-SEM) images demonstrated AgNPs nanoscale with an average size of 40-50 nm. AgNPs showed considerable potential to eliminate both trophozoite and cyst stages of the parasite; trophozoites readily appeared to absorb silver nanoparticles, while cyst stages suffered destruction in their resistant walls.

1. Introduction

Acanthamoeba castellani is an opportunistic free-living protozoan that is the leading cause of a severe vision infection in mammals called *Acanthamoeba keratitis* (AK) **[1]**. A potentially blinding cornea infection that has gained global attention due to an annual rise in reports **[2]**. In 1930, the scientist Castellani discovered *Acanthamoeba* **[3]**. These organisms blossom in hot tubs, swimming pools, and ponds. They can reside as latent cysts or active trophozoites **[4]**. It enters the eyes, nasopharyngeal mucosa, skin, through contact lenses (CL), surgical instruments, drainages, dust, filth, air, dialysis machines, and sediments. As soon as it enters the eye, it primarily affects the corneal epithelium, enters the stroma, and penetrates the corneal nerves, causing necrosis, beginning to destroy target cells quickly **[5]**. Ring-like stromal infiltrates and corneal lesions are the characteristic features of this infection. The ring infiltrates could be seen as transparent in the center of the cornea, leading to loss of vision **[6]**. Furthermore, **[7]** state that this pathogen is an uncommon corneal infection that might harm eyesight if left undiagnosed and untreated. It is frequently resistant to standard eye treatments **[8]** because of its cyst stage double walls, which make it resistant to a range of environmental stressors, such as harsh conditions like hunger, pH, heat, osmolality, dryness, chlorination, antimicrobial substances, and PHMB resistance **[9]**. Misdiagnosing infections as fungal or viral keratitis leads to delayed treatment and potential visual loss. The most successful treatment known is a mixture of hexamidine and propamidine isethionate or chlorhexidine digluconate, as no single medicine has been identified. Unfortunately, Prolonged therapy with these medicinal substances is highly harmful to the eyes **[10]**. The development of medications to treat this infection is insufficient because of the rarity of the disease and the lack of knowledge among **[11]**. Unfortunately, the amoebic activity of diamides and biguanides, which are typically used as the first line of therapy, is quite intrusive because of the Prolonged treatment that increases corneal toxicity and promotes amoebae encystament **[7]**. There is an urgent need to develop innovative treatments that are low toxicity to the eye but have high effects against all stages of *Acanthamoeba* spp. Furthermore, Many compounds failed to be effective against *Acanthamoeba* spp because they were difficult to penetrate the brain barrier, and the cyst stage's rigid structure made it resistant to extreme conditions **[12]**. Recent studies have paid little attention to the identification of nanoparticles and their use in AK treatments, as they do with many other parasites. Several nanoparticles (NPs) have been

tested *in vitro* to assess their effectiveness as antimicrobial **[13]** and insecticidal **[14]**. Few studies have examined the effectiveness of nanoparticles against amoebic protozoans, such as *Acanthamoeba*. Nanoparticles, particularly silver nanoparticles (AgNPs), have been investigated in vitro for their effectiveness against harmful microbes, and they are developing as potential antimicrobial, antidiabetic, Antioxidant, antibiofilm and antiviral agents **[15-18]**. Unfortunately, there is limited research on the effectiveness of nanoparticles against amoebic protozoans, such as *Acanthamoeba*. Silver nanoparticles' ability to kill parasitic organisms has been examined in helminths such as *Echinococcus granulosus* and trematodes such as *Schistosoma japonicum* **[19, 20]**. and hematophagous vectors like *Haemaphysalis* sp., *Anopheles* sp., and *Culex* sp. **[21]**. The AgNPs are demented the anti-protozoal activity against *Giardia intestinalis*, *Leishmania* spp., *Toxoplasma gondii*, *Entamoeba histolytica*, *Plasmodium* spp. and *Cryptosporidium parvum* **[22, 23]**. It was also detected by **[24, 25]** that AuNPs can exhibit anti-protozoal action. Our research is a novel investigation of the *in vitro* effect of silver nanoparticle on *Acanthamoeba castellani*.

2. Materials and Methods

2.1. Isolation of *Acanthamoeba*

An eye examination involved a thorough evaluation with the slit lamp. Seventy-eight patients' corneal smears were collected from different hospitals in Basrah province, Iraq, using a sterile cotton swab that was rolled from one side to the other. Samples were taken from the eye and lower conjunctiva and examined under a light microscope, as **[26]** stated. Finally, they were microscopically examined using the wet-mount technique.

2.2. Cultivation, examination, staining, and classification

The positive isolates were grown in petri dishes contain the PYG medium (1.0% agar, 0.75% w/v yeast extract, 0.75% w/v proteose peptone, and 1.5% w/v glucose), the medium was autoclaved and supplied with 10 mg/mL gentamicin and penicillin at 27°C then incubated at 30-32 **[27]**. Strains were subcultured twice, then examined under a light microscope. The wet mount technique includes adding two drops of *Acanthamoeba* suspension, then spreading the drops out on a glass slide, and covering them with a coverslip **[28]**.

The count for *Acanthamoeba* cells was performed by adding sterile PBS saline solution to the media, followed by collecting the *Acanthamoeba* cells by centrifugation (5 minutes at 2000 rpm). Finally, the cells were washed twice using sterile PBS solution **[29]**, and were counted using a Neubauer hemocytometer. The vitality of *Acanthamoeba* cells was measured

using a 1:1 ratio of the "Trypan Blue" dye (0.4%) added to the wet mount prepared previously **[30]**. The staining of *Acanthamoeba* cells was conducted using different stains, including methylene blue and 0.1% eosin. One drop of each stain was added to the previously prepared wet mount, then the coverslip was put over it. The slides were examined under a light microscope with a 100X magnification. Finally, the genus was morphologically categorized by **[31]**.

2.3. The aqueous extract R. officinalis leaf preparation

The dry leaves of *R. officinalis* were collected from the local markets of Basrah city, Iraq. The leave powder was prepared using electrical grinder. Next, 3 g of the leave powder were added to a conical flask contains a 100 ml of a sterile distilled water (D.W) following the method described by **[32]**. The blend was then heated using stirred hot plate at 30 °C for 15 min. After that, the extract was filtered using filter paper and stored at 4 °C until subsequent use.

2.4. Silver nanoparticles preparation

Silver nanoparticles were synthesized using *R. officinalis* leaf extract **[33]**. The protocol was conducted by firstly preparing a fresh aqueous solution of silver nitrate (AgNO3) (0.001 M). In a 250 ml glass clean beaker, 95 ml of water was put on the hot plate and vigorously stirred for one minute. After that, 5 ml of *R. officinalis* leaf extract was gradually added and left for mixing for 30 min. The reaction mixture was left in a dark place for 24 hours to reduce the silver salt and synthesize silver nanoparticles fully. After overnight incubation, the synthesized AgNPs was centrifuged at 10.000rpm for 15 min, and the pellet was collected and washed twice with DW. The pellet was then dried, and weighed then 1 ml of DW was added to prepare suspension and then stored in a dark place at room temperature. This solution was used as a stock solution to prepare seven serial dilutions of AgNPs using distilled water.

2.5. Silver nanoparticles characterization

To investigate the silver nanoparticle characterization, a UV-Vis spectrophotometer within wavelengths of 200-800 nm was employed to obtain the peak of AgNPs. Further, the chemical constitutions of AgNP surface or *R. officinalis* extract were analyzed using an FTIR device (BRUKER, the University of Basrah, chemistry department) with the wavelengths of 400 and 4000 cm-1. Zeta potential (HORIBA) was utilized to discover the potential charge of the silver nanoparticle surface with Conductivity: 0.066 mS/cm and Electrode Voltage: 3.8 V.

In addition, Field Emission Scanning Electron Microscopy (FESEM) (ZEISS), (MIRA III, Czech Republic) was employed to obtain silver nanoparticle images with a magnification of 100.00 kx, a resolution unit at ETH 5.00 kV, and a window of electrons of 8.3mm **[34]**.

2.6. The in vitro effect of AgNPs on the *Acanthamoeba* parasite

Acanthamoeba cyst and trophozoites, with concentration 6×105 cells/ml, were treated in vitro with different concentrations of green-synthesized AgNPs (100, 50, 25, 12.5, 6.2, 3.1, and 1.6 µg /ml) for periods of 2, 4, and 6 minutes. A control samples were prepared using distilled water and set for the above periods of time. Amoebicidal activity was calculated using the percentage of cell death. Cell counting was done after each experiment using a direct light microscope and a haemocytometer **[35]**. The experiment was made in triplicate, with three independent experiments, and conditions were regulated similarly. The standard deviation and mean values were computed.

2.7. Drug extract exposure

Acanthamoeba cyst and trophozoites (4×10 5 cells/ml) were treated with Polyhexamethylene Biguanide PHMB (0.02%) by adding a drop of this drug in distinct tubes for a period of, 2, 4, and 6 minutes and then incubated at 25°C. The cell viability was evaluated. Incubation with water was used for the control group. Quantification was used after PHMB exposure; using a Hemocytometer, all experiments were repeated 3 times **[36]**.

2.8. Statistical analysis

All statistical analyses in this study were conducted using IBM SPSS Statistics version 27 and Microsoft Excel 2019 for data analysis, visualization, and result validation.

3. Results

3.1. Acanthamoeba isolation from AK patients

Infected patients have been suffering from different symptoms depending on the infection stage (as illustrated in Figure 1). The clinical features of the early stage of AK included reddish eyes, inflamed conjunctivae, tears, strong corneal infection, and severe pain (Figure 1 (1)). Furthermore, white ring stromal infiltrates and corneal lesions in the second stage of infection were detected (Figure 1 (2)). Another patient showed a marked corneal injury in the late stage of AK, showing that the cornea was relatively translucent, yielding to vision loss (Figure 3 (3)).

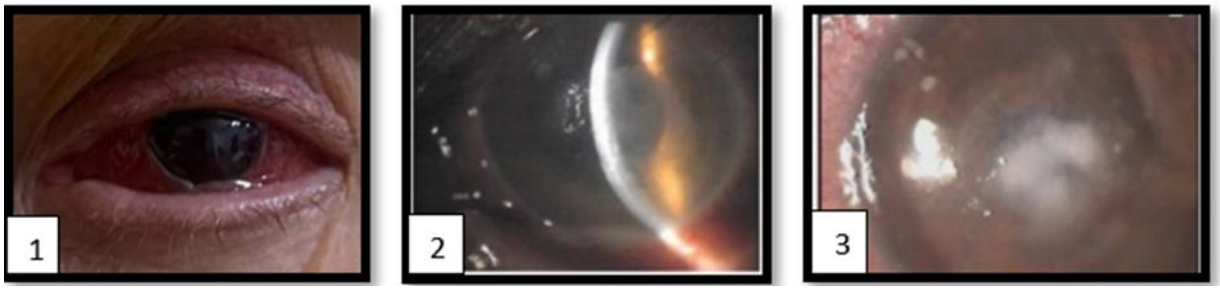

Figure 1. The infected eyes with *Acanthamoeba keratitis*.1- The first stage of infection shows an inflamed eye, inflammation of the conjunctiva, and congested sclera. 2- showing abscess and ring infiltrate. 3- Diffusion and infiltration of the cornea.

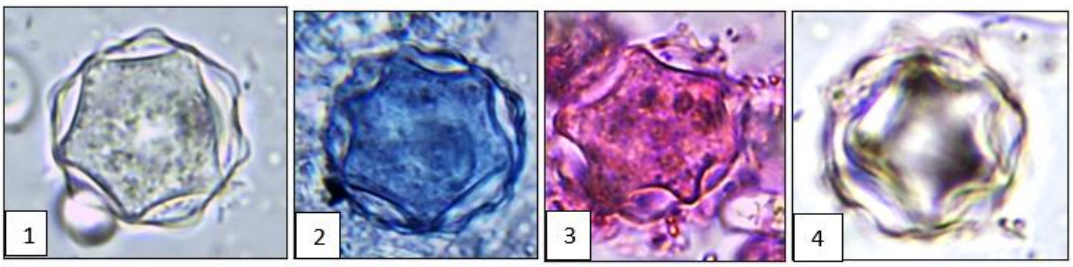

Figure 2. Microscopic image of *Acanthamoeba castellanii* cyst 1-unstained 2-trypan blue stained 3-eosin stained 4-methylene blue stained

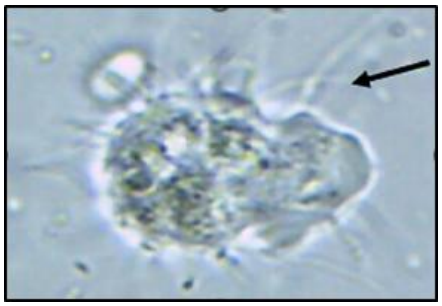

Figure 3. Microscopic image of *Acanthamoeba castellanii* trophozoite showing the acanthopoda (arrow).

3.2. Silver nanoparticles synthesis

Figure 4 exhibit the colour conversion from of the combination of brown colored *R. officinalis* leaf extract (1) and AgNO3 solution (2) from light yellowish brown (3) to dark greenish brown (4) post 30 minutes of the combination at 40°C and then to a greenish dark brown after 24 hours of the combination at 25°C in a dark place.

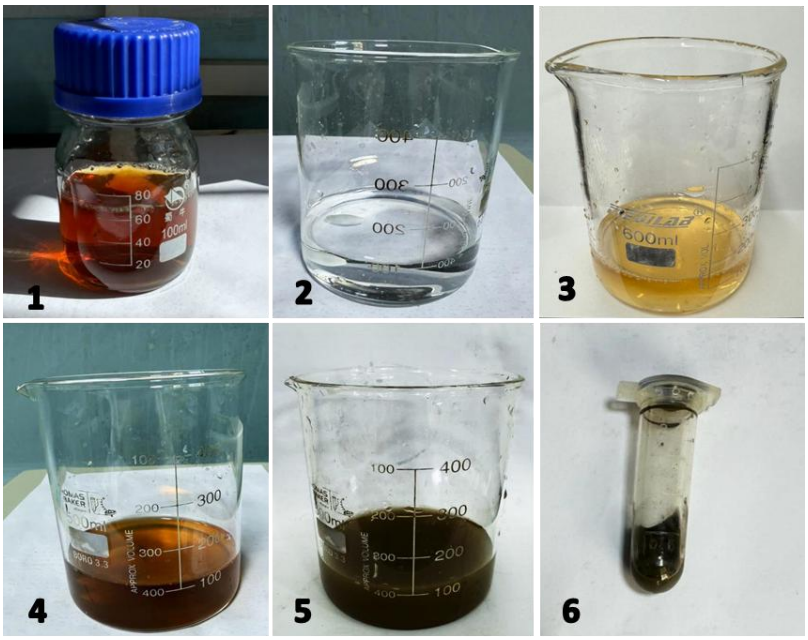

Figure 4. Color change during silver nanoparticle synthesis. 1) plant extract, 2) silver nitrate salt (AgNO3), 3) plant extract and AgNO3 after 0 min of the incubation, 4) plant extract and AgNO3 after 15 min of the incubation, 5) plant extract and AgNO3 after 24 hour and 6) silver nanoparticles after centrifugation

3.3.Silver nanoparticles characterization

3.3.1. UV-vis spectrophotometer analysis

Figure 5 exemplifies the optical absorbance spectra of AgNPs. The peak of the absorbance was concentrated at a wavelength of 455 nm.

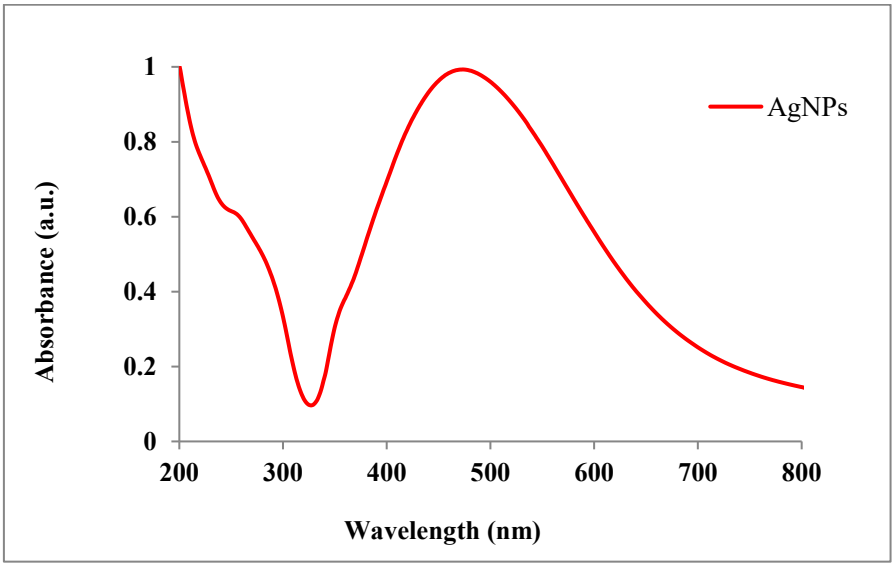

Figure 5. UV–vis spectrophotometer absorption of AgNPs

3.3.2. Fourier Transform Infrared Spectroscopy (FTIR) analysis

Figure 6 reveals the outcome of Fourier transform infrared test of AgNPs utilizing *R. officinalis* leaf extract. It has been getting a broad maximal peak at a wavelength of 3280.85 cm-1, which suggests the presence of a hydroxyl group (-OH) of the aqueous plant extract. Moreover, the FTIR investigation revealed another four peaks located at different wavelengths (1638.71 cm^{-1}, 1257.68 cm^{-1}, 1118.66 cm^{-1}, and 948.43 cm^{-1}).

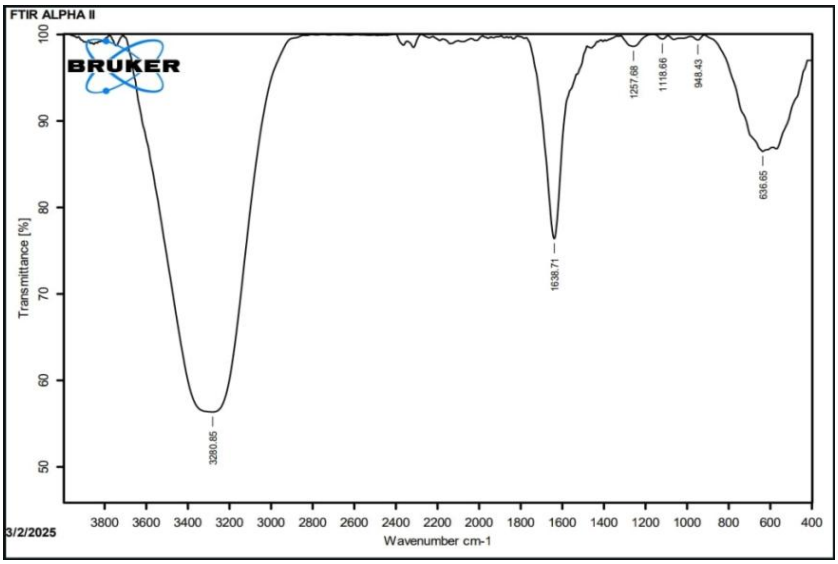

Figure 6. FTIR analysis of AgNPs

3.3.3. Zetasizer analysis

The size distribution of AgNPs was investigated using Zetasizer Nano ZS (Malvern, physics department, University of Basrah, Iraq). Figure 7 indicates the size distribution of AgNPs with nanoparticle number. The analysis showed significant details, including that the size of 99.8% of nanoparticles was about 25.70 nm, while only 0.2% of nanoparticles had a size of 103 nm; this led to the size average (Z-Average) being found to be 106.3 (d.nm). The value of Polydispersity index (PDI) was at 0.516, and the standard deviation was 5.113.

Table 1. Size distribution of AgNPs

The variable	The value
Size (d.nm)	25.70
Z-average (d.nm)	106.3
PDI	0.516
The standard deviation	5.113
The intercept	0.78
The quality of result	Good

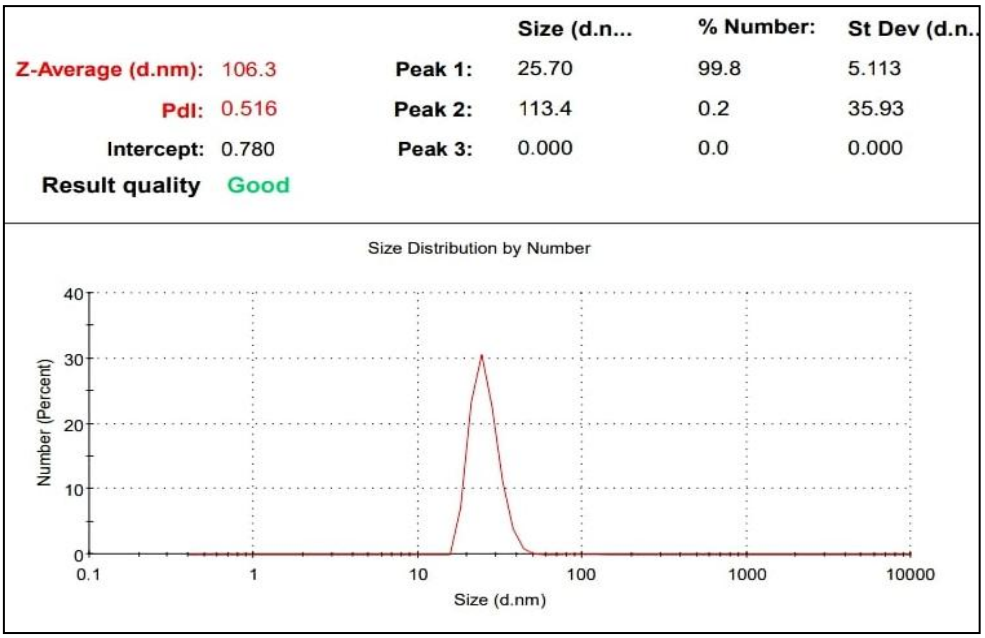

Figure 7. Zetasizer analysis of AgNPs

3.3.4. X-ray diffraction (XRD) analysis

The chemical construction of nanoparticle surfaces, the atomic disposition, the size, and orientation of nano-crystals were inquired into using the X-ray diffraction (XRD) test. Figure 6 appears the XRD analysis of AgNPs with clear linear broad peaks at 32.18°, 38.08°, 45.78°, 55.94°, 66.33°, 73.78°, and 79.18°. These positions of peaks correspond to 122, 111, 200, 142, 220, 311, and 112 values of AgNPs XRD, respectively.

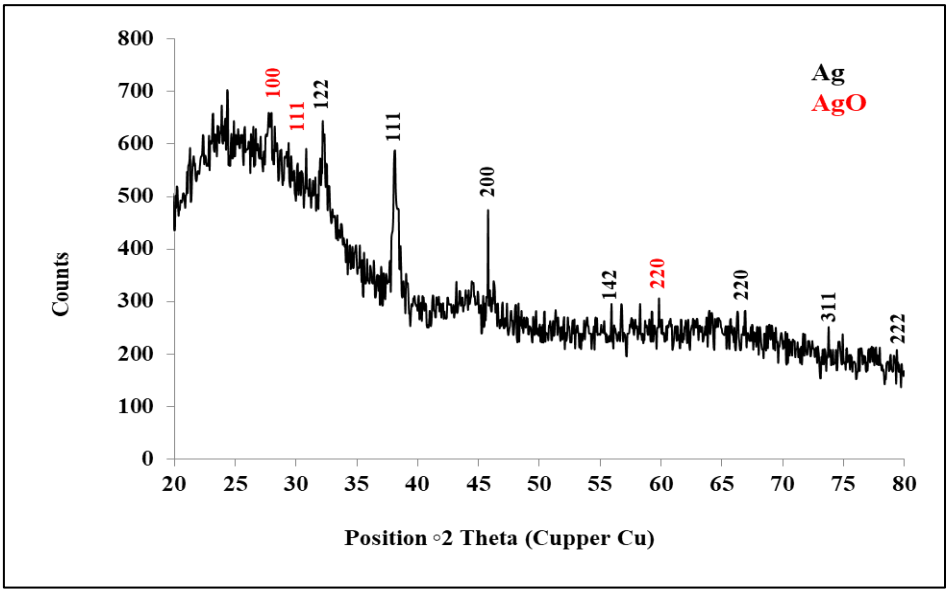

Figure 8. X ray diffraction (XRD) analysis of AgNPs

3.3.5. Zeta potential analysis

Figure 9 exhibits zeta potential analysis of AgNPs, which was found to be one peak at -41.7mV.

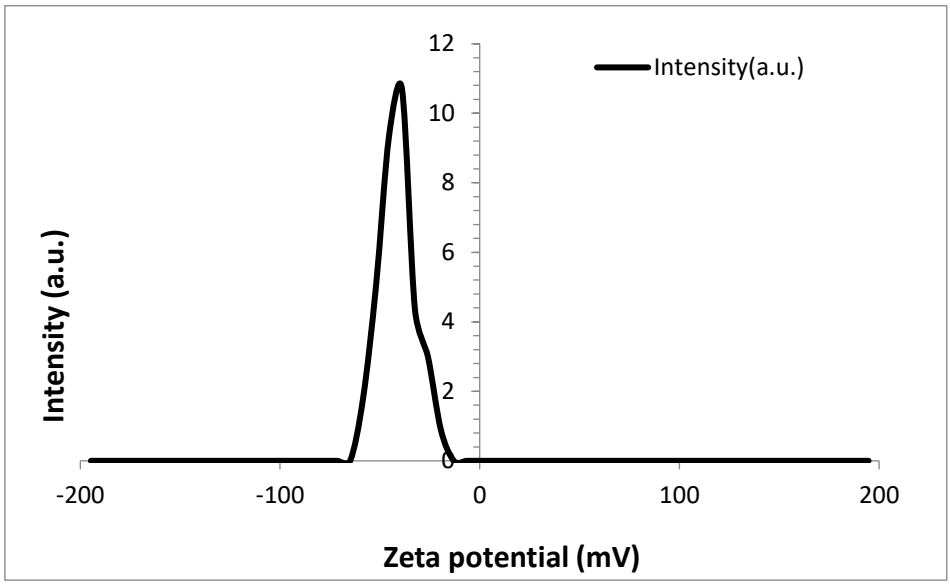

Figure 9. Zeta potential analysis of AgNPs

Table 2. Zeta potential analysis of AgNPs

Parameter	Calculation Results
Peak No. 1	-41.7 mV -0.000323 cm2/Vs
Peak No. 2	--- mV --- cm2/Vs
Peak No. 3	--- mV --- cm2/Vs
Zeta Potential (Mean)	-41.7 mV
Electrophoretic Mobility Mean	-0.000323 cm2/Vs

3.3.6. Field Emission-Scanning Electron Microscope (FE-SEM) images

Silver nanoparticle images were captured using a Field Emission Scanning Electron Microscope (FESEM), as established in Figure 10. The image presented a visible structure, shape, and size for AgNPs that appeared in a spherical character with small sizes of 40-50 nm.

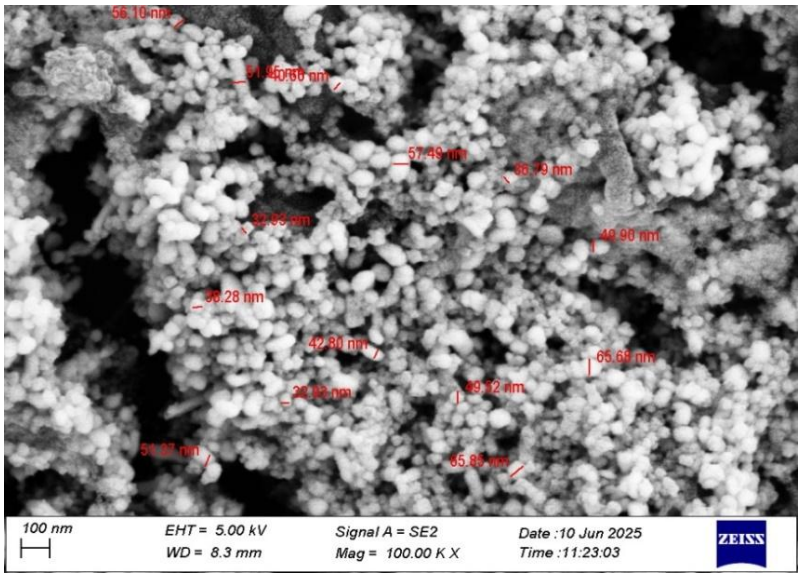

Figure 10. FE-SEM image of AgNPs

3.4 AgNPs' activity and cytotoxicity

One of the primary goals of nanoparticles used in this study is to examine their therapeutic potential against *Acanthamoeba* spp, and validate their efficacy. Through in vitro investigation, it was found that these compounds had strong lethal characteristics against *Acanthamoeba*. Indicated that trophozoites yielded varying results based on the type of NP utilized.

Table 3 shows the analysis of the effect of different concentrations (1.6–100 µg/ml) and exposure times (2, 4, 6 minutes) on the trophozoite stage of the parasite, comparing the effectiveness of the tested substance with the PHMB treatment and the control group. The results indicate that there are clear significant differences between the concentrations, as shown by LSD and statistically significant values ($p< 0.05$) at all times, confirming the cumulative effect of concentration and time on inhibition of the cyst stage.

In a 2-minute exposure period, high concentrations (100, 50, 25, 12.5 and 6.2 µg/ml) maintained killing rates close to 100% with no significant differences between them (all with the letters "a" and "b"), indicating the efficiency of the nanoparticles in this short period. Further, the effectiveness of the AgNPs began to decrease at the concentrations of 3.2 and 1.6 µg/ml with mortality rates of 67.7 ± 1.5 c and 41 ± 2.1 d, respectively. However, AgNPs at 3.2 and 1.6 µg/ml showed a statistically significant differences in mortality efficacy compared to the PHMB treatment that exhibited a mortality rate of 23.3 ± 1.5 e. In addition, in a 4-minute exposure period, all concentrations of 100, 50, 25 and 12.5 showed complete mortality rates of the trophozoites at 100% with no significant differences. The concentration of 6.2,

3.1, and 1.6 µg/ml continued to show a mortality of 92 ± 3.6 b, 78 ± 0.6 c and 60 ± 2.3 d, respectively, with a gradual decrease depending on the concentration. However, interestingly, still the lowest concentration able to cause a statistically significant mortality of 60 ± 2.3 d, compared to the drug of PHMB that showed 34.7 ± 2.6 e. Further, results indicate increased effectiveness of the AgNPs in conjunction with the length of the exposure time (a 4-minute) compared to a 2-minute exposure period. Further, in a 6-minute exposure period, the results showed higher efficacy compared to the previous two times. The effect of AgNPs was high (99.3% ± 0.3% a) at a concentration of 6.2 µg/ml, also, the concentrations of 3.1 and 1.6 µg/ml exhibited mortality rates of 72% ± 13.6% c and 70.6% ±1.2%c, respectively, with no differences. As can be seen, these lowest concentrations of AgNPs exhibited a statistically significant mortality rate in comparison to PHMB treatment, which recorded (45% ± 2.3% d).

Figure 11 shows the change in the percentage of trophozoite stage destruction after treatment at different concentrations of AgNPs and for increasing exposure periods (2, 4, 6 minutes). The histograms show that the length of the exposure time plays a fundamental role in enhancing the inhibitory effect of AgNPs, as the 6-minute exposure duration (blue column) caused the complete elimination of the parasite at almost all concentrations, with a mortality rate of almost 100%, indicating a very high effectiveness of the AgNP in this period. In 4-minute exposure period (red column), a gradual increase in the percentage is observed with high concentration, from 1.6 µg/ml to 100 µg/ml, with relative stability after 12.5 µg/ml. 2-minute data (striped column) show relatively low mortality rates, especially at low concentrations (1.6–6.2 µg/ml), reflecting the limited effect of the substance at short exposure duration.

Table 4 shows the effectiveness of different concentrations (1.6-100 µg/ml) of AgNPs under study in inhibiting the parasite cyst under the influence of three exposure periods (2, 4, 6 minutes), compared to the PHMB treatment and the control group. It is noted from the statistical values of the LSD test that the differences between the concentrations were significant at each exposure time ($p < 0.05$).

Table 3: Analysis of the effect of AgNP at different concentrations and exposure times on the trophozoite stage, with comparison with the effectiveness of PHMB treatment and control

Time	Concentration	Trophozoite Stage	$LSD_{0.05}$
2 min	100	100 ± 0 a	0.0173*
	50	100 ± 0 a	
	25	96.7 ± 3.3 b	
	12.5	95 ± 2.6 b	
	6.2	85 ± 2.6 b	
	3.1	67.7 ± 1.5 c	
	1.6	41 ± 2.1 d	
	PHMB	23.3 ± 1.5 e	
	Control	0 ± 0 f	
4 min	100	100 ± 0 a	0.0399*
	50	100± 0 a	
	25	100 ± 0 a	
	12.5	100 ± 0 a	
	6.2	92 ± 3.6 b	
	3.1	78 ± 0.6 c	
	1.6	60 ± 2.3 d	
	PHMB	34.7 ± 2.6 e	
	Control	0 ± 0 f	
6 min	100	100 ± 0 a	0.0265*
	50	100 ± 0 a	
	25	100 ± 0 a	
	12.5	100 ± 0 a	
	6.2	99.3 ± 3 a	
	3.1	72 ± 13.6 b	
	1.6	70.6 ± 1.2 c	
	PHMB	45 ± 2.3 d	
	Control	0 ± 0 e	

Values are expressed as (Mean ± standard error (S.E.)

*Significant difference between groups (p value < 0.05)

In each period of time, different litters mean there is statistically significant different.

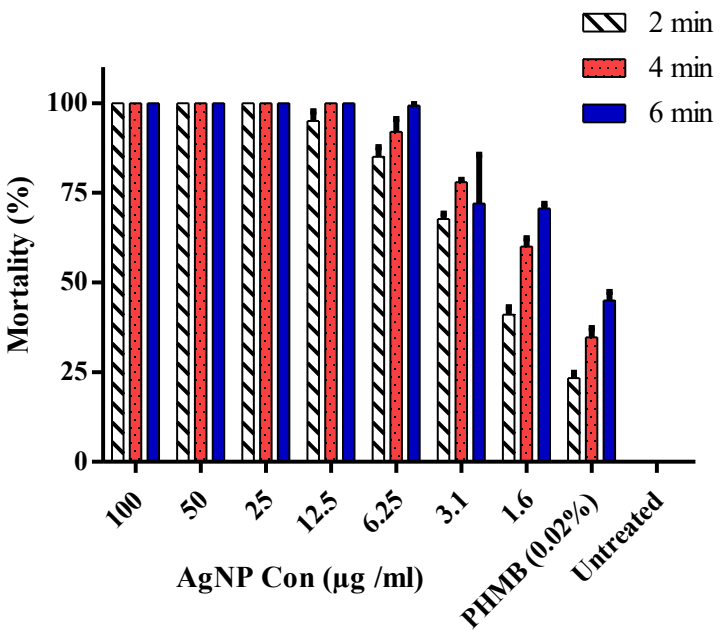

Figure 11. Percentage of trophozoite phase mortality after treatment at different concentrations of AgNPs and for multiple exposure periods (2, 4, 6 minutes)

In 2 minutes, the inhibitory effects at 100 µg/ml of AgNPs were (100 ± 0 a), while at 50 25 µg/ml were 99.3 ± 02.8 b and 81 ± 1 b with no significant differences between them. The mortality of cysts was gradually declining with decreasing the concentrations. In addition, 56.7 ± 2.8 c of cysts was destroyed from 12.5 µg/ml of AgNPs. However, AgNPs destroyed 21.3 ± 1.5 e of cysts with 3.1 µg/ml of AgNPs, with no statistically significant difference compared to the PHMB treatment (23.3 ± 1.5 e), while the control group was devoid of any activity (0 ± 0 f).

Further, in 4 minutes, the effects from the concentrations of 100, 50 µg/ml were found to be 100%± 0.0a. Although the mortality rates decreased slightly at concentrations of 50, 25, and 12.5, the rate of mortality was still high. Interestingly, the effect of AgNPs at 3.1 µg/ml on cysts (37 ± 3.1 e) was also similar to the PHMB treatment (34.7 ± 2.6 e) with no statistically significant differences, which enhances the feasibility of the comparison.

In addition, in 6 minutes, the differences were significantly increased, with a concentration of 50 µg/ml, the mortality of cysts was 89.3 ± 0.3 b. Remarkably, the concentration of 3.1 µg/ml showed a high efficacy of 45.7 ± 1.8 e close to the PHMB treatment (45 ± 2.3 e), highlighting the cumulative temporal efficiency of AgNPs. The lowest concentrations showed less efficacy in inhibiting the cysts, with the lowest mortality rate recorded at 1.6 µg/ml (28 ± 0.5 f).

Table 4. Effect of different concentrations of AgNPs and exposure times on cyst stage, with comparison with the effectiveness of PHMB treatment and control

Time	AgNP concentration (µg/ml)	Cyst Stage	$LSD_{0.05}$
2 min	100	100 ± 0 a	0.0285*
	50	99.3 ± 2.8 b	
	25	81 ± 1 b	
	12.5	56.7 ± 2.8 c	
	6.2	41.7 ± 2.2 d	
	3.1	21.3 ± 1.5 e	
	1.6	17 ± 0.2 f	
	PHMB	23.3 ± 1.5 e	
	Untreated (Control)	0 ± 0 f	
4 min	100	100 ± 0 a	0.0319*
	50	100 ± 0 a	
	25	85 ± 1.5 b	
	12.5	65.7 ± 2.4 c	
	6.2	47.7 ± 0.7 d	
	3.1	37 ± 3.1 e	
	1.6	21.4 ± 0.6 f	
	PHMB	34.7 ± 2.6 e	
	Untreated (Control)	0 ± 0 f	
6 min	100	100 ± 0 a	0.0174*
	50	100 ± 0 a	
	25	89.3 ± 0.3 b	
	12.5	75.7 ± 2.8c	
	6.2	56 ± 3.5 d	
	3.1	45.7 ± 1.8 e	
	1.6	28 ± 0.5 f	
	PHMB (0.02%)	45 ± 2.3 e	
	Untreated (Control)	0 ± 0 f	

Values inside the table are expressed as (Mean ± standard error (S.E.)

*Significant difference between groups (p value < 0.05)

In each period of time, different litters mean there is statistically significant different.

Figure 12 shows the change in the percentage of cyst stage destroying after treatment with different concentrations of AgNPs and for increasing exposure periods (2, 4, 6 minutes). The graph shows that the cyst phase is less responsive to the treatment than the trophozoite stage, where the percentage of depreciation is significantly reduced at low concentrations, while it increases with increasing exposure duration, as the histograms show that the length of the exposure time plays a fundamental role in enhancing the inhibitory effect of AgNPs,

At concentrations of 100 and 50 µg/ml, the three time curves showed distinct responses, with the cumulative time effect evident. The exposure time of 6 minutes (blue column)

recorded a mortality rate of 100% at higher concentrations, while this percentage was low in a time of 2 minutes (striped column). In 4-minute exposure period (red column), a gradual increase in the percentage is observed with high concentration. The 2-minute data (striped column) show relatively low mortality rates, especially at low concentrations (1.6–6.2 µg/ml), reflecting the limited effect of the substance at short exposure duration.

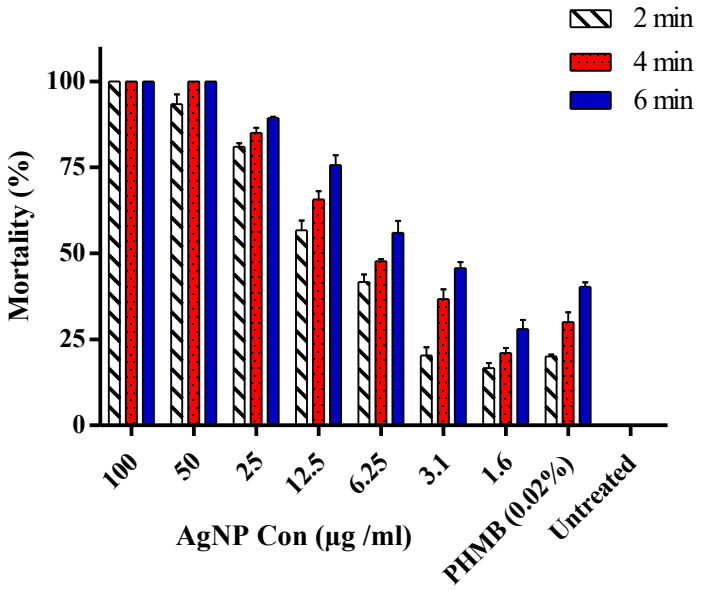

Figure 12. Percentage of cyst stage mortality after treatment at different concentrations of AgNPs and for multiple exposure periods (2, 4, 6 minutes)

Furthermore, Figure 13 shows the microscopic images of *A. castellanii* cysts after 6 minutes of incubation with different concentrations of AgNPs, as well as the control without treatment. As can be seen that AgNPs induced clear morphological changes in *A. castellanii* cysts, which found to be dose-dependent. The cyst in the image A showed small morphology change after 6 minutes of the incubation compared to the cyst in the control image, however, this change became clearer in the cyst of the image B. It was clearly observed that AgNPs at 3.1 and 6.2 µg/ml were concentrated in the cytoplasm of the cyst of images B and C respectively, which appeared as brown colour (red arrows). Moreover, with increasing AgNP concentrations, 12.5, 25 and 50 µg/ml (Images D, E, and F, respectively), the morphology of the cysts lost its significant arms. It became irregularly shaped and further developed to brown pigmentation, resulting from increased AgNP concentration within the cysts. Interestingly, at the highest concentration, 100 µg/ml of AgNPs (Image G), *A. castellanii* cysts lost their walls

and were finally exposed to apoptosis; thus, they do not exhibit a distinctive shape, due to the disturbance by the AgNPs; however, a remnant of the cyst can be seen (yellow arrows).

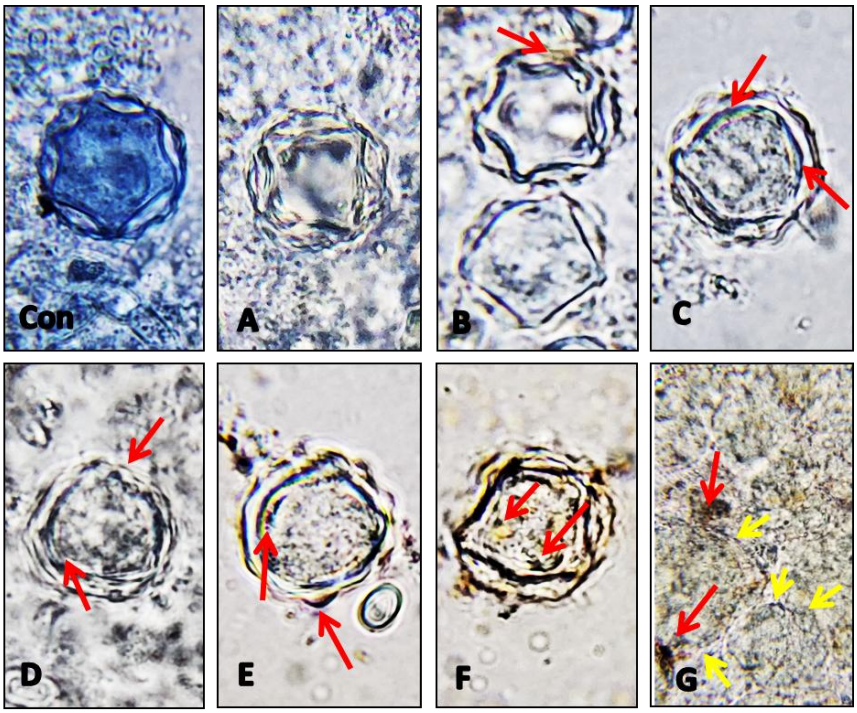

Figure 13. Microscopic images of *Acanthamoeba castellanii* cysts after 6 minutes of the incubation with A 1.6 µg/ml, B) 3.1 µg/ml, C) 6.2 µg/ml, D) 12.5 µg/ml, E) 25 µg/ml, F) 50 µg/ml and G) 100 µg/ml of AgNPs, in addition to Con: control without treatment with AgNPs. The red arrows manifest the AgNPs inside the cyst stage which increases with rising the concentration of AgNPs nanoparticles

4. Discussion

4.1 *Acanthamoeba* isolation from AK patients

Different strains are important for detecting the morphological details of clinical specimens' phases for identifying the isolated pathogenic strain **[7]**. The results of this study showed that the stain of methylene blue is effectively visualized the morphological details of *Acanthamoeba* species stages, making differentiation between species straightforward, whereas eosin was adequate for staining *Acanthamoeba* cysts. These results agree with the data of **[37]**. Finally, the protozoan was classified morphologically depending on the presence of 6 arms in cyst stages, and it was related to the genus *Acanthamoeba* castellani, as indicated by **[32]**. Also, the trophozoite stage contained fine acanthopodia, which were the characteristic feature of the genus.

4.2 Silver nanoparticles synthesis

The images in Figure 2 confirm the Ag^1 ion reduction to Ag^0 during the synthesis. The resulting Ag0 is gathered to form tiny clusters, which are then converted into silver nano-sized particles. These outcomes are close to the prior studies **[38, 39]** The presentation of final color of silver nanoparticles was expected as a result of a surface Plasmon Resonance phenomenon **[40]**. It has been indicated that the chemical substances accord in the *R. officinalis* leaves contain different active substances that effectively reduce and cap of nanoparticles during the green synthesis process **[41, 42]**.

4.3. Silver nanoparticles characterization

The result of UV-Vis absorbance are almost identical to earlier research, revealing that silver nanoparticle absorption peaks are between 420 and 450 nm **[43-45]**. These absorption peaks have been shown to result from the resonance of silver nanoparticle surface electrons **[46, 47]**. The UV–vis spectrophotometer is the first technique that can be applied to identify various classes of nanoparticles **[48]** Moreover, the SPR peaks give deep facts regarding their specific sizes, as it has been demonstrated that the nanoparticles with a small size could exhibit an absorbance at 410-420nm compared to the large ones. A study of **[49]** demonstrated that the AgNPs with 15.3nm in size exhibited an optical absorption peak of 412 nm. Hence, the AgNPs in this study showed an absorbance peak at 455 nm, which could be desired within a size range of more than 15.3 nm, which could be confirmed by further examination.

Furthermore, the peaks of FTIR (1638.71 cm^{-1}, 1257.68 cm^{-1}, 1118.66 cm^{-1}, and 948.43 cm^{-1}), are related to the interaction between the silver ions and the active groups of *R. officinalis* plant, which explicate the AgNP synthesis. The last peak at 636.65 cm^{-1} is related to the Ag ions. These outcomes are coordinated with earlier records **[42, 50]**.

Overall, Zetasizer analysis quality was found to be good, which indicates that AgNPs are spherical and entirely monodispersed [**[1]**. Table 1 summarises the data shown in Figure 5 regarding the size distribution of AgNPs. The current results are identical to those of previous studies **[2, 3]**.

This study found that the data of X-ray diffraction (XRD) analysis are comparable to the positions of θ2 XRD motifs of the Joint Committee on Powder Diffraction Standards (JCPDS) data of the number (00-001-1167). A study of **[53]** revealed the same positions of peaks.

Furthermore, the peaks at 27.73°, 30.23°, and 59.83° were found to be correlated with 100, 111, and 220 of XRD values of AgONPs, which correspond to the JCPDS data card of (01–076-1489) **[54]**.

The results of Zeta potential analysis were similar to previous that record by **[45, 55]**. It is well known that the value of zeta potential (± 30 mV) is desired for the stabilization of nanoparticles **[56]**. The value of the zeta potential of AgNPs could be related to the charge of organic molecules of the plant extract that cover nanoparticles during the synthesis process. The value of zeta potential is a factor in the cytotoxicity of nanoparticles against *Acanthamoeba*, as they can enter the cysts and trophozoites and produce apoptosis. Furthermore, all captured images of AgNPs showed that the particles were monodispersed, with no evidence of obvious aggregation. These results are agreed with various previous studied **[57-59]**.

4.4. AgNPs' activity and cytotoxicity

These results of AgNPs' activity and cytotoxicity suggest that the effectiveness of the AgNPs is directly related to the duration of exposure, and that average concentrations can achieve a significant effect when time increases. These findings are consistent with recent studies on the role of time and concentration as critical factors in controlling stages such as the trophozoite, where previous experiments have shown that the cyst requires longer exposure or higher doses to achieve efficacy equivalent to that observed against the trophozoite stage **[60-62]**.

The mortality patterns of trophozoite phase suggest a direct relationship between focus and effectiveness at short exposure periods, while an increase in exposure time enables a strong effect even at medium concentrations. These observations support the results of the previous table, reinforcing the hypothesis of the combined cumulative effect of time and concentration. Such an effect has been documented in previous studies that have shown that resistance requires a longer exposure time to achieve the optimal effect **[60-62]**.

These results of the cyst stage mortality are consistent with recent literature that Cyst has a cellular structure that is more exposed to inhibitory agents than Cyst, making it more susceptible to chemical treatments at relatively short exposure periods **[60, 62]**. Further, the results also These results also support the hypothesis that simultaneous use of active concentration with appropriate exposure duration is critical in eliminating the parasite's living phases.

The results of this study suggest that the AgNPs have inhibited both stages of the parasite and assisted in the breakdown of the wall integrity. They also slowed and suppressed the trophozoite stage's growth, proving that they exhibit strong killing properties.

Using a different concentration of AgNPs has been demonstrated to destroy and inhibit the cyst walls, considerably obstructing the formation of trophozoites and inhibiting their encystation. This result matches the study of **[63]** which showed that AgNPs have a pivotal effect on the lipid structure of the plasma membrane of microorganisms, leading to its disintegration and exhausting the intracellular ATP levels.

Furthermore, the findings suggest that AgNP treatment may decrease *Acanthamoeba castellani* growth by triggering trophozoites autophagy and death through ingestion and internalisation of AgNPs. This is agrees to the study of **[64]** that showed that AgNPs lead to the oxidative destruction within cells and likely interact with cell membrane proteins, releasing silver ions that reduce the production of RNA and DNA. Also, a study on *Candida albicans* found that AgNPs caused oxidative stress-induced cell death by accumulating reactive oxygen species (ROS) and affecting membranes, ergosterol content, cellular morphology, and ultrastructural components **[65]**.

The AgNPs reduced the number of trophozoites and cysts, and their effects were highly fatal. Compared to the control, the treated with AgNPs demonstrated total suppression and destruction. This is similar to the study by **[66]** which found a substantial dose dependent reduction in adherence and metabolic activity after treatment with AgNPs against the environmental strain of *Acanthamoeba*.

5. Conclusions

There aren't many studies on how well AgNP works against *Acanthamoeba*. However, they are advantageous against infections caused by free-living amoebae due to their numerous medical benefits, in addition to their antiviral, antibacterial, and antiprotozoal properties. The present study investigations have indicated that combining AgNPs with plant metabolites may be a potential technique for amoebicidal action against A. castellanii in both stages. This technique can be used to treat *Acanthamoeba* infections. Furthermore, the minimum value of AgNP that was used in vitro for both stages of *Acanthamoeba* was more effective in killing than the PHMB used.

6. References

[1] Z. A. Abdulbaki, S. A. Alsamir, and N. A. A. Almansour, "The use of *Matricaria chamomilla* aqueous extract as a treatment of mouse eyes experimentally infected with *Acanthamoeba castellanii*," *Al-Kunooze Scientific Journal*, vol. 11, pp. 20–35, 2025. https://doi.org/10.36582/rpvxf598

[2] J. McKelvie, M. Alshiakhi, M. Ziaei, D. V. Patel, and C. N. McGhee, "The rising tide of *Acanthamoeba* keratitis in Auckland, New Zealand: a 7-year review of presentation, diagnosis and outcomes (2009–2016)," *Clinical & Experimental Ophthalmology*, vol. 46, no. 6, pp. 600–607, 2018. https://doi.org/10.1111/ceo.13166

[3] P. A. Fuerst, G. C. Booton, and M. Crary, "Phylogenetic analysis and the evolution of the 18S rRNA gene typing system of *Acanthamoeba*," *Journal of Eukaryotic Microbiology*, vol. 62, no. 1, pp. 69–84, 2015. https://doi.org/10.1111/jeu.12186

[4] B. R. Esboei *et al.*, "Genotyping and phylogenic study of *Acanthamoeba* isolates from human keratitis and swimming pool water samples in Iran," *Parasite Epidemiology and Control*, vol. 11, p. e00164, 2020. https://doi.org/10.1016/j.parepi.2020.e00164

[5] A. Salameh, N. Bello, J. Becker, and T. Zangeneh, "Fatal granulomatous amoebic encephalitis caused by *Acanthamoeba* in a patient with kidney transplant: a case report," *Open Forum Infectious Diseases*, Oxford University Press, vol. 2, no. 4, p. ofv104, 2015. https://doi.org/10.1093/ofid/ofv104

[6] J. Lorenzo-Morales, N. A. Khan, and J. Walochnik, "An update on *Acanthamoeba* keratitis: diagnosis, pathogenesis and treatment," *Parasite*, vol. 22, p. 10, 2015. https://doi.org/10.1051/parasite/2015010

[7] J. Lorenzo-Morales, C. M. Martín-Navarro, A. López-Arencibia, F. Arnalich-Montiel, J. E. Piñero, B. Valladares, *et al.*, "*Acanthamoeba* keratitis: an emerging disease gathering importance worldwide?," *Trends in Parasitology*, vol. 29, no. 4, pp. 181–187, 2013. https://doi.org/10.1016/j.pt.2013.01.006

[8] J. Nagington, P. Watson, T. Playfair, J. McGill, B. Jones, and A. M. Steele, "Amoebic infection of the eye," *The Lancet*, vol. 304, no. 7896, pp. 1537–1540, 1974. https://doi.org/10.1016/s0140-6736(74)90285-2

[9] W. Mitsuwan, S. Sangkanu, C. Romyasamit, C. Kaewjai, T. O. Jimoh, M. de Lourdes Pereira, *et al.*, "*Curcuma longa* rhizome extract and Curcumin reduce the adhesion of *Acanthamoeba triangularis* trophozoites and cysts in polystyrene plastic surface and contact lens," *International Journal for Parasitology: Drugs and Drug Resistance*, vol. 14, pp. 218–229, 2020. https://doi.org/10.1016/j.ijpddr.2020.11.001

[10] C. Sanchez and A. Gustavo, "Molecular manipulation and new antimicrobial identification in *Acanthamoeba* spp.," 2021. https://doi.org/10.48730/j6bt-9m18

[11] Y.-J. Wang, C.-H. Chen, J.-W. Chen, and W.-C. Lin, "Commensals serve as natural barriers to mammalian cells during *Acanthamoeba castellanii* invasion," *Microbiology Spectrum*, vol. 9, no. 2, pp. e00512-21, 2021. https://doi.org/10.1128/Spectrum.00512-21

[12] M. R. Mungroo, R. Siddiqui, and N. A. Khan, "War of the microbial world: *Acanthamoeba* spp. interactions with microorganisms," *Folia Microbiologica*, vol. 66, no. 5, pp. 689–699, 2021. https://doi.org/10.1007/s12223-021-00889-7

[13] R. Aguilar-Garay, L. F. Lara-Ortiz, M. Campos-López, D. E. Gonzalez-Rodriguez, M. M. Gamboa-Lugo, J. A. Mendoza-Pérez, *et al.*, "A comprehensive review of silver and gold nanoparticles as effective antibacterial agents," *Pharmaceuticals*, vol. 17, no. 9, p. 1134, 2024. https://doi.org/10.3390/ph17091134

[14] M. J. Alyusif, I. J. Albandar, and N. A. A. Almansour, "Comparative analysis of the insecticidal activity of Biogenic Zinc Oxide Nanoparticles, Iron Oxide Nanoparticles and *Piper nigrum* fruits extract against 1st instar larva of House fly (*Musca domestica*) (Diptera: Muscidae)," *Journal of Bioscience and Applied Research*, vol. 11, pp. 243–259, 2025. https://doi.org/10.21608/jbaar.2024.326210.1090

[15] I. Albandar, S. Jabbar, T. K. Ibrahim, O. A. Radhi, and Z. S. Mbalaha, "Advances of Nanotechnology in Eradication Bacterial Infectious Diseases: A Recent Review," *Kirkuk Journal of Science*, vol. 19, 2024. https://doi.org/10.32894/kujss.2024.145530.1131

[16] O. K. Awote, A. B. Ojekale, M. I. Kazeem, A. G. Adeyemo, J. O. Igbalaye, R. Ilesanmi, *et al.*, "Antidiabetic, antioxidant, antiglycation, and anti-inflammatory potentials of green-synthesized silver nanoparticles using *Telfairia occidentalis* leaf and stem aqueous extracts," *Letters in Applied NanoBioScience*, vol. 13, p. 41, 2024. https://doi.org/10.26538/tjnpr/v8i9.23

[17] A. E.-R. R. El Shanshoury, S. Z. Sabae, W. A. El Shouny, H. E. Elsaied, H. M. Badr, and A. M. Abo-Shady, "Biomimetic Synthesis of Silver Nanoparticles Using New Aquatic Species of *Bacillus*, *Alcaligenes*, and *Paenibacillus* and their Potential Antibiofilm Activity against Biofilm-Forming *Escherichia coli*," *Letters in Applied NanoBioScience*, vol. 12, p. 127, 2023. https://doi.org/10.33263/LIANBS124.127

[18] D. Srisrimal, S. Krishnan, and A. Thirunavukkarasu, "In vitro virucidal activity of silver nanoparticles against H1N1 Influenza a virus and herpes simplex virus-1," *Letters in Applied NanoBioScience*, vol. 12, p. 136, 2023. https://doi.org/10.33263/LIANBS124.136

[19] E. Rahimi, J. van den Berg, and W. Veen, "Facilitating student-driven constructing of learning environments using Web 2.0 personal learning environments," *Computers & Education*, vol. 81, pp. 235–246, 2015. https://doi.org/10.1016/j.compedu.2014.10.012

[20] Y. Cheng, X. Chen, W. Song, Z. Kong, P. Li, and Y. Liu, "Contribution of silver ions to the inhibition of infectivity of *Schistosoma japonicum* cercariae caused by silver

nanoparticles," *Parasitology*, vol. 140, no. 5, pp. 617–625, 2013. https://doi.org/10.1017/S0031182012002211

[21] C. Jayaseelan, A. A. Rahuman, A. V. Kirthi, S. Marimuthu, T. Santhoshkumar, A. Bagavan, *et al.*, "Novel microbial route to synthesize ZnO nanoparticles using *Aeromonas hydrophila* and their activity against pathogenic bacteria and fungi," *Spectrochimica Acta Part A: Molecular and Biomolecular Spectroscopy*, vol. 90, pp. 78–84, 2012. https://doi.org/10.1016/j.saa.2012.01.006

[22] C. Panneerselvam, K. Murugan, M. Roni, A. T. Aziz, U. Suresh, R. Rajaganesh, *et al.*, "Fern-synthesized nanoparticles in the fight against malaria: LC/MS analysis of *Pteridium aquilinum* leaf extract and biosynthesis of silver nanoparticles with high mosquitocidal and antiplasmodial activity," *Parasitology Research*, vol. 115, no. 3, pp. 997–1013, 2016. https://doi.org/10.1007/s00436-015-4828-x

[23] S. G. Azad and H. C. Özyurt, "In vitro and in vivo effects of green-synthesized silver nanoparticles against *Giardia lamblia* infection," *Archives of Razi Institute*, vol. 79, no. 1, pp. 218–225, 2024. https://doi.org/10.32592/ARI.2024.79.1.218

[24] G. Benelli, "Gold nanoparticles–against parasites and insect vectors," *Acta Tropica*, vol. 178, pp. 73–80, 2018. https://doi.org/10.1016/j.actatropica.2017.10.021

[25] A. Roy, "A review on the alkaloids an important therapeutic compound from plants," *International Journal of Plant Biology*, vol. 3, no. 2, pp. 1–9, 2017. https://doi.org/10.37628/IJPB.V3I2.199

[26] M. B. Aldin, N. M. Ardalan, and K. A. Jassim, "Isolation and molecular characterization of *Acanthamoeba* spp. from Iraqi patients with Keratitis," *Baghdad Science Journal*, vol. 21, no. 6, 2024. https://doi.org/10.21123/bsj.2023.8059

[27] I. H. Hameed, G. J. Mohammed, and S. A. Kamal, "A review: Uses and Pharmacological activity of *Matricaria chamomilla*," *Indian Journal of Public Health Research & Development*, vol. 9, no. 3, pp. 200–205, 2018. https://doi.org/10.5958/0976-5506.2018.00209.7

[28] N. M. El-Sayed, K. A. Ismail, S. A.-E.-G. Ahmed, and M. H. Hetta, "In vitro amoebicidal activity of ethanol extracts of *Arachis hypogaea* L., *Curcuma longa* L. and *Pancratium maritimum* L. on *Acanthamoeba castellanii* cysts," *Parasitology Research*, vol. 110, no. 5, pp. 1985–1992, 2012. https://doi.org/10.1007/s00436-011-2727-3

[29] Z. A. Abdulbaki, S. A. Alsamir, and N. A. A. Almansour, "In Vitro Effect of Aqueous Extract of *Moringa oleifera* Plant on *Acanthamoeba* Spp," *Journal of Medical Research and Health Sciences*, vol. 6, no. 9, pp. 2763–2765, 2023. https://doi.org/10.52845/JMRHS/2023-6-9-5

[30] G. Bernardes, D. S. Alves, D. C. Silva, *et al.*, "Viability test exclusively is not adequate to evaluate the T4 *Acanthamoeba* keratitis' treatment," *Journal of Microbiology & Experimentation*, vol. 8, no. 1, pp. 1–5, 2020. https://doi.org/10.15406/jmen.2020.08.00278

[31] F. C. Page, "Re-definition of the genus *Acanthamoeba* with descriptions of three species," *The Journal of Protozoology*, vol. 14, no. 4, pp. 709–724, 1967. https://doi.org/10.1111/j.1550-7408.1967.tb02066.x

[32] A. Abebe, K. T. Hilawea, A. Mekonnen, G. T. Tigineh, B. Sitotaw, M. Liyew, *et al.*, "Assessment on antioxidant activity of the aqueous leaf extracts of *Combretum microphyllum* and the effect of Co (II)-leaf extract complex on antibacterial activity of leaf extracts of the plant material," *Scientific African*, vol. 18, p. e01432, 2022. https://doi.org/10.1016/j.sciaf.2022.e01432

[33] A. M. Awwad, N. M. Salem, and A. O. Abdeen, "Green synthesis of silver nanoparticles using carob leaf extract and its antibacterial activity," *International Journal of Industrial Chemistry*, vol. 4, p. 29, 2013. https://doi.org/10.1186/2228-5547-4-29

[34] V.-D. Hodoroaba, S. Rades, T. Salge, J. Mielke, E. Ortel, and R. Schmidt, "Characterisation of nanoparticles by means of high-resolution SEM/EDS in transmission mode," *IOP Conference Series: Materials Science and Engineering*, IOP Publishing, vol. 109, p. 012006, 2016. https://doi.org/10.1088/1757-899X/109/1/012006

[35] L. Chomicz, D. B. Conn, M. Padzik, J. P. Szaflik, J. Walochnik, P. J. Zawadzki, *et al.*, "Emerging threats for human health in Poland: pathogenic isolates from drug resistant *Acanthamoeba* keratitis monitored in terms of their in vitro dynamics and temperature adaptability," *BioMed Research International*, vol. 2015, p. 231285, 2015. https://doi.org/10.1155/2015/231285

[36] C. S. P. Mafra, L. C. Carrijo-Carvalho, A. M. Chudzinski-Tavassi, F. M. de Carvalho Taguchi, A. S. Foronda, F. R. de Souza Carvalho, *et al.*, "Antimicrobial action of biguanides on the viability of *Acanthamoeba* cysts and assessment of cell toxicity," *Investigative Ophthalmology & Visual Science*, vol. 54, no. 9, pp. 6363–6372, 2013. https://doi.org/10.1167/iovs.13-11990

[37] F. Berrilli, M. Montalbano Di Filippo, I. Guadano-Procesi, M. Ciavurro, and D. Di Cave, "*Acanthamoeba* Sequence Types and Allelic Variations in Isolates from Clinical and Different Environmental Sources in Italy," *Microorganisms*, vol. 12, no. 3, p. 544, 2024. https://doi.org/10.3390/microorganisms12030544

[38] L. Pardo, J. Arias, and P. Molleda, "Preparation of synthesized silver nanoparticles from extract of rosemary leaves (*Rosmarinus officinalis* L.) and its used as a perservative," *La*

Granja: Revista de Ciencias de la Vida, vol. 35, pp. 46–58, 2022. https://doi.org/10.17163/lgr.n35.2022.04

[39] D. K. Takcı, M. S. Ozdenefe, and S. Genc, "Green synthesis of silver nanoparticles with an antibacterial activity using *Salvia officinalis* aqueous extract," *Journal of Crystal Growth*, vol. 614, p. 127239, 2023. https://doi.org/10.1016/j.jcrysgro.2023.127239

[40] Z. M. Ayad, O. M. S. Ibrahim, and L. W. Omar, "Biosynthesis and characterization of silver nanoparticles by *Silybum marianum* (silymarin) fruit extract," *Advances in Animal and Veterinary Sciences*, vol. 7, no. 2, pp. 122–130, 2019. https://doi.org/10.17582/journal.aavs/2019/7.2.122.130

[41] M. G. Rahbardar and H. Hosseinzadeh, "Therapeutic effects of rosemary (*Rosmarinus officinalis* L.) and its active constituents on nervous system disorders," *Iranian Journal of Basic Medical Sciences*, vol. 23, no. 9, pp. 1100–1112, 2020. https://doi.org/10.22038/ijbms.2020.45269.10541

[42] I. Albandar and Z. S. Mbalaha, "Investigating The Anticancer and Antioxidant Activity of Silver Nanoparticles from *Rosmarinus officinalis*, in vitro Analysis," *Basrah Journal of Science*, vol. 42, no. 2, pp. 501–519, 2024. https://doi.org/10.29072/basjs.20240221

[43] B. A. Kumar, N. Ahmed, and S. Jamal, "Biosynthesis and Characterization of Silver Nanoparticles (AgNPs) with Jacalin, a Lectin from Jackfruit Seeds and its Antiproliferative Effects on HeLa Cancer Cells," *Letters in Applied NanoBioScience*, vol. 13, no. 3, p. 106, 2024. https://doi.org/10.33263/LIANBS133.106

[44] M. Ansari, S. Ahmed, A. Abbasi, M. T. Khan, M. Subhan, N. A. Bukhari, *et al.*, "Plant mediated fabrication of silver nanoparticles, process optimization, and impact on tomato plant," *Scientific Reports*, vol. 13, p. 18048, 2023. https://doi.org/10.1038/s41598-023-45038-x

[45] I. Albandar, O. A. Radhi, S. A. Al-Saadi, and M. A. Mahdi, "Eco-Friendly Synthesis of Silver Nanoparticles Using *Prosopis farcta* Fruit Extract and Evaluate Their Biological Applications," *Pakistan Journal of Life and Social Sciences*, vol. 22, no. 1, p. 00266, 2024. https://doi.org/10.57239/pjlss-2024-22.1.00266

[46] S. Singh, A. Bharti, and V. K. Meena, "Green synthesis of multi-shaped silver nanoparticles: Optical, morphological and antibacterial properties," *Journal of Materials Science: Materials in Electronics*, vol. 26, no. 6, pp. 3638–3648, 2015. https://doi.org/10.1007/s10854-015-2881-y

[47] R. H. Salih, W. K. Obead, and A. M. Al-Shammari, "Synergistic anticancer effect of silver nanoparticles and Measles virus vaccine strain against hormone-dependent and-independent breast cancer cells," *Nanomedicine Research Journal*, vol. 7, no. 1, pp. 37–48, 2022. https://doi.org/10.22034/nmrj.2022.01.003

[48] W. Qi, Y. Tian, D. Lu, and B. Chen, "Detection of glutathione in dairy products based on surface-enhanced infrared absorption spectroscopy of silver nanoparticles," *Frontiers in Nutrition*, vol. 9, p. 982228, 2022. https://doi.org/10.3389/fnut.2022.982228

[49] A. K. Tomer, T. Rahi, D. K. Neelam, and P. K. Dadheech, "Cyanobacterial extract-mediated synthesis of silver nanoparticles and their application in ammonia sensing," *International Microbiology*, vol. 22, no. 1, pp. 49–58, 2019. https://doi.org/10.1007/s10123-018-0026-x

[50] F. A. Qais, A. Shafiq, H. M. Khan, F. M. Husain, R. A. Khan, B. Alenazi, *et al.*, "Antibacterial Effect of Silver Nanoparticles Synthesized Using *Murraya koenigii* (L.) against Multidrug-Resistant Pathogens," *Bioinorganic Chemistry and Applications*, vol. 2019, p. 4649506, 2019. https://doi.org/10.1155/2019/4649506

[51] M. Danaei, M. Dehghankhold, S. Ataei, F. Hasanzadeh Davarani, R. Javanmard, A. Dokhani, *et al.*, "Impact of particle size and polydispersity index on the clinical applications of lipidic nanocarrier systems," *Pharmaceutics*, vol. 10, no. 2, p. 57, 2018. https://doi.org/10.3390/pharmaceutics10020057

[52] M. Wolie, E. Kassa, and A. Teferi, "Green Synthesis, Characterization of Silver Nanoparticles using *Justicia Schimperiana* Leaf Extract and its Antibacterial Activity," *Letters in Applied NanoBioScience*, vol. 14, p. 82, 2023. https://doi.org/10.33263/LIANBS142.082

[53] M. M. Shanwaz and P. Shyam, "Synthesis of silver nanoparticles from *Vitex negundo* plant by green method and their bactericidal effects," *Letters in Applied NanoBioScience*, vol. 12, no. 2, pp. 59–62, 2022. https://doi.org/10.33263/LIANBS122.059

[54] M. I. Rahmah, R. S. Sabry, and W. J. Aziz, "Preparation of superhydrophobic Ag/Fe2O3/ZnO surfaces with photocatalytic activity," *Surface Engineering*, vol. 37, no. 10, pp. 1320–1327, 2021. https://doi.org/10.1080/02670844.2021.1948156

[55] M. Pisárčik, M. Lukáč, J. Jampílek, F. Bilka, A. Bilková, Ľ. Pašková, *et al.*, "Silver nanoparticles stabilized with phosphorus-containing heterocyclic surfactants: Synthesis, physico-chemical properties, and biological activity determination," *Nanomaterials*, vol. 11, no. 8, p. 1883, 2021. https://doi.org/10.3390/nano11081883

[56] A. Aruna, R. Nandhini, V. Karthikeyan, and P. Bose, "Synthesis and characterization of silver nanoparticles of insulin plant (*Costus pictus* D. Don) leaves," *Asian Journal of Biomedical and Pharmaceutical Sciences*, vol. 4, no. 34, pp. 1–6, 2014. https://doi.org/10.15272/ajbps.v4i34.532

[57] D. Wang, L. Wang, Q. Sun, J. Qu, and X. Zhang, "Size Optimization of Spherical Silver Nanoparticles Synthesized with Baicalin and Sodium Dodecyl Sulfate Using Response

Surface Methodology," *Journal of Physics: Conference Series*, IOP Publishing, vol. 2679, p. 012002, 2024. https://doi.org/10.1088/1742-6596/2679/1/012002

[58] I. Albandar, "Biogenic Synthesis of *Solanum nigrum* Mediated Silver Nanoparticles and study its antioxident and Antibacterial Effects," *Letters in Applied NanoBioScience*, vol. 14, p. 145, 2025. https://doi.org/10.33263/LIANBS143.145

[59] L. Niu, Z. Lin, W. Hu, D. Yang, H. Shen, and F. Guo, "Silver nanoparticles derived from *Streptomyces* sp. YJD18 with multifunctional biomedical applications," *Scientific Reports*, vol. 15, p. 18139, 2025. https://doi.org/10.1038/s41598-025-02925-9

[60] A. K. Sharma, A. K. Swami, M. Saran, and M. Mathur, "Synthesis of tungsten nanoparticles for their biomedical application," *International Journal of Pharmaceutical Sciences and Research*, vol. 11, no. 8, pp. 4070–4077, 2020. https://doi.org/10.13040/IJPSR.0975-8232.11(8).4070-77

[61] I. Goze, A. Alim, S. Dag, B. Tepe, and Z. A. Polat, "In vitro amoebicidal activity of *Salvia staminea* and *Salvia caespitosa* on *Acanthamoeba castellanii* and their cytotoxic potentials on corneal cells," *Journal of Ocular Pharmacology and Therapeutics*, vol. 25, no. 4, pp. 293–298, 2009. https://doi.org/10.1089/jop.2008.0132

[62] R. Cedillo-Rivera, B. Chávez, A. González-Robles, A. Tapia, and L. Yépez-Mulia, "In vitro effect of nitazoxanide against *Entamoeba histolytica*, *Giardia intestinalis* and *Trichomonas vaginalis* trophozoites," *Journal of Eukaryotic Microbiology*, vol. 49, no. 3, pp. 201–208, 2002. https://doi.org/10.1111/j.1550-7408.2002.tb00523.x

[63] C.-N. Lok, C.-M. Ho, R. Chen, Q.-Y. He, W.-Y. Yu, H. Sun, *et al.*, "Proteomic analysis of the mode of antibacterial action of silver nanoparticles," *Journal of Proteome Research*, vol. 5, no. 4, pp. 916–924, 2006. https://doi.org/10.1021/pr0504079

[64] M. M. Rohde, C. M. Snyder, J. Sloop, S. R. Solst, G. L. Donati, D. R. Spitz, *et al.*, "The mechanism of cell death induced by silver nanoparticles is distinct from silver cations," *Particle and Fibre Toxicology*, vol. 18, p. 37, 2021. https://doi.org/10.1186/s12989-021-00430-1

[65] P. Chand, K. Narula, R. Vs, S. Sharma, S. Kumari, N. Mondal, *et al.*, "Mechanistic Insights into Cellular and Molecular Targets of Zinc Oxide Quantum Dots (ZnO QDs) in Fungal Pathogen, *Candida albicans*: One Drug Multi-Targeted Therapeutic Approach," *ACS Infectious Diseases*, vol. 10, no. 6, pp. 1914–1934, 2024. https://doi.org/10.1021/acsinfecdis.3c00562

[66] A.-L. Grün, P. Scheid, B. Hauröder, C. Emmerling, and W. Manz, "Assessment of the effect of silver nanoparticles on the relevant soil protozoan genus *Acanthamoeba*," *Journal of Plant Nutrition and Soil Science*, vol. 180, no. 5, pp. 602–613, 2017. https://doi.org/10.1002/jpln.201700277

تأثير جسيمات الفضة النانوية في المختبر على طفيلي *Acanthamoeba castellani*

زينب صلاح المياحي ، انتصار البندر*، شيماء عبد الرزاق السامر

قسم علوم الحياة، كلية العلوم، جامعة البصرة، البصرة، العراق

المستخلص

التهاب القرنية هو عدوى قرنية تهدد الرؤية، تسببها الطفيلية الأولية "*Acanthamoeba castellani*"، ولا يوجد لها حاليًا أي علاج فعال وآمن سواءً للإنسان أو الحيوان. ونتيجةً لذلك، هنالك ثمة حاجة ماسة إلى عوامل مضادة للأميبا أكثر فعالية وأمانًا. تهدف الدراسة إلى تحديد تأثير جسيمات الفضة النانوية (AgNPs) على السلالات السريرية لأنواع *Acanthamoeba*. جُمعت 78 عينة من قرنية مرضى التهاب القرنية (AK) *Acanthamoeba Keratitis* باستخدام مسحة معقمة من مستشفيات مختلفة في محافظة البصرة بالعراق. صُنعت جسيمات الفضة النانوية (AgNPs) باستخدام مستخلص أوراق إكليل الجبل، واستُخدمت بتركيزات تسلسلية لتقييم سميتها الخلوية في المختبر. أظهرت جسيمات الفضة النانوية ذروة امتصاص عند 455 نانومتر. حدد تحليل FTIR المكونات الكيميائية في المستخلص التي تساهم في تخليق جسيمات الفضة النانوية وتثبيت السطح. أظهرت جسيمات الفضة النانوية (AgNPs) حجمًا قدره 25.70 نانومترًا ومتوسط Z قدره 106.3 نانومترًا باستخدام Zeta sizer. كان تحليل حيود الأشعة السينية (XRD) مُشابهًا لمواقع معياري الفضة Ag وأكسيد الفضة AgO. كشف تحليل جهد زيتا عن ذروة عند -41.7 مللي فولت. أظهرت صور المجهر الإلكتروني الماسح بالانبعاث الميداني (FE-SEM) جسيمات الفضة النانوية بحجم نانوي يبلغ متوسطة 40-50 نانومترًا. أظهرت جسيمات الفضة النانوية قدرة كبيرة على القضاء على كلٍ من مرحلتي الطفيليات الخضرية والكيسات؛ إذ بدا أن الطفيليات الخضرية تمتص جسيمات الفضة النانوية بسهولة، بينما عانت مرحلتي الكيس من التدمير في جدرانهما المقاومة.

الكلمات المفتاحية: *Acanthamoeba castellanii*، تكنولوجيا النانو، دقائق الفضة النانوية، الجسيمات النانوية المضادة للطفيليات، *Rosmarinus officinalis*.